Available online at www.CivileJournal.org

Civil Engineering Journal

(E-ISSN: 2476-3055; ISSN: 2676-6957)

Vol. 12, No. 03, March, 2026

Flexural Response of RC Beams with Variable-Width Prestressed and Non-Prestressed CFRP Plate Strengthening

Yasir Safaa Al-Khafaji [1*], Alaa Hussein Al-Zuhairi [1]

[1] *Department of Civil Engineering, Faculty of Engineering, University of Baghdad, 10071 Baghdad, Iraq.*

Received 29 October 2025; Revised 12 February 2026; Accepted 17 February 2026; Published 01 March 2026

Abstract

This experimental research was conducted to quantify the combined effect of the external bonded Carbon Fiber Reinforced Polymer (CFRP) plate width and prestressing on the flexural performance of reinforced concrete (RC) beams in terms of strength improvement. Seven beams (one control and six strengthened) were subjected to two-point loading tests. The experimental methodology consisted of the testing of three different widths of the CFRP plates (25, 40, and 60 mm) in non-prestressed and prestressed conditions. Prestressing was accomplished by tensioning the plates to 23% of the CFRP tensile strength using a novel, locally developed mechanical anchorage system, which is one of the key experimental contributions that distinguishes this study from investigations that vary only one parameter. Results showed that although non-prestressed CFRP increased the ultimate load by 22.4%-32.3%, prestressed strengthening had superior gains ranging from 29.8% to 67.6%. Prestressed beams had similar ultimate deflections, which greatly enhanced crack control. Notably, prestressing successfully changed the critical failure mode from partial debonding to beneficial CFRP rupture, validating the efficiency of the anchorage system and CFRP-stress utilization. The results show that increasing plate width improves capacity and that suggests that the combination of width and prestress parameters must be optimized for balanced structural design.

Keywords: Reinforced Concrete Beams; CFRP Plates; Prestressed CFRP; Flexural Strengthening; Plate Width; Load–Deflection Behavior; Mechanical Anchorage System.

1. Introduction

Deterioration of reinforced concrete (RC) infrastructure caused by corrosion of conventional steel reinforcement is an ongoing global challenge. The American Society of Civil Engineers (ASCE) 2021 Report Card, which graded the state of global infrastructure at C-, draws attention to the fact that a significant percentage of the existing stock does not meet modern performance and durability requirements [1]. Specifically, post-tensioned (PT) concrete girders exhibit high susceptibility to strand corrosion and concrete cover damage due to aggressive environmental conditions and accidental impacts, hence impairing load-bearing capacity, resulting in excessive deformation, and demanding costly repair or replacement cycles [1, 2]. Externally bonded carbon fiber reinforced polymer (CFRP) laminates have emerged as a desirable solution for strengthening and rehabilitation of RC members due to their high strength-to-weight ratio, corrosion resistance, and ease of installation [1]. While non-prestressed CFRP flexural strengthening has been widely used, premature debonding and spalling of concrete cover can result in less-than-optimal use of the composite, leading to less-than-optimal strength gains and economic disadvantages [3]. On the other hand, CFRP strengthening alone or along with other methods has been proven to have an important effect on increasing the load-carrying capacity and ductility of RC members, especially those made with low-strength concrete [4].

Against this background, extensive research has been conducted on prestressed CFRP systems in order to utilize a higher percentage of the material's tensile capacity and improve serviceability performance. Early experimental studies on the failure modes of reinforced concrete (RC) beams strengthened with prestressed carbon fiber reinforced polymer

* Corresponding author: yasser.hussein2201m@coeng.uobaghdad.edu.iq

https://doi.org/10.28991/CEJ-2026-012-03-09

plates (CFRP) were conducted by Garden & Hollaway [5], who found that non-prestressed specimens failed mainly due to plate buckling and concrete cover failure, whereas prestressed specimens tended to fail by CFRP rupture. In a subsequent study, nine RC beams with prestressing levels varying from 17.5% to 46.6% of the CFRP tensile strength showed failure by laminate fracture without debonding and exhibited significantly improved flexural response [6]. Barros [7] presented a near-surface-mounted (NSM) prestressing system capable of applying 20% prestressing to CFRP strips and demonstrated better load capacity and serviceability than surface-bonded systems. Numerical analyses by Deng et al. [8] and Woo et al. [3] showed that prestressed CFRP–RC composite beams have higher ultimate moment capacity and stiffness, particularly when failure is governed by concrete crushing rather than CFRP rupture, and they developed cross-section analysis models for predicting cracking, yielding, and ultimate states.

Further contributions have investigated the effects of strengthening layout, prestress level, and anchorage configuration on flexural behavior and fatigue performance. Finite element simulations reported in Altaee [9], showed that positioning prestressed plates closer to the beam edges can increase flexural strength by about 11% compared to mid-span bonding. Kang et al. [10] found that prestress levels of 20%, 30%, and 40% improved strength and ductility while reducing crack widths. The fatigue crack growth rate of prestressed CFRP tendon-reinforced metallic beams was found to be significantly reduced due to the presence of prestress [11]. Rezazadeh et al. [12], comparing fully bonded, partially bonded, and hybrid systems, concluded that hybrid configurations provide a favorable balance between load-carrying capacity and ductility, although excessively high prestress can reduce the effectiveness of deflection control. Fatigue studies on prestressed NSM systems have shown stable behavior up to two million cycles, which was found to be relatively independent of both concrete strength and tendon length [13]. Anchorage-free or self-anchored prestressing concepts have also been investigated. Yang et al. [14] demonstrated up to a 30% increase in CFRP tensile utilization without mechanical anchorages, thereby reducing interfacial stresses and the risk of debonding, while Jeong et al. [15] found that untaped CFRP bars maintain their characteristic stiffness and load capacity under cyclic loading with enhanced ductility. Low-cost mechanical anchorage solutions, such as aluminum anchorage systems capable of safely delivering more than 50% prestress while protecting tendons from premature debonding, have been proposed to enhance practical applicability [16–18].

At the structural system level, prestressed CFRP has been implemented in castellated beams, bridge girders, and composite structural members. Hashim & Al-Zuhairi [17] demonstrated enhanced flexural strength in castellated beams with a trapezoidal external post-tensioning strand profile, achieving improvements of up to 20.7%. A self-anchored technique utilizing up to 81% of the CFRP tensile capacity was reported to significantly increase stiffness and improve crack control [18]. Rogowski & Kotynia [19] compared prestressing with CFRP and shape memory alloys (SMA), highlighting the mechanical superiority of CFRP while noting concerns related to anchorage efficiency and cost. Liu et al. [20] studied full-scale bridge beams strengthened with prestressed CFRP plates and demonstrated improved cracking resistance, deflection control, and ultimate capacity; parametric finite element analyses were also conducted to clarify the effects of plate length and number of plates. Tang [21] summarized recent developments and emphasized the need to optimize anchoring and prestressing systems to minimize debonding failures. Complementary studies on prestressed basalt FRP (BFRP) laminates suggested that, at similar pretension levels, BFRP laminates may exhibit improved deformation characteristics compared with CFRP [22]. Shen et al. [23] reported significant improvements in ultimate and yield strengths (47.9% and 39.8%, respectively) and a 21.7% increase in stiffness in steel–concrete composite beams strengthened with a 3 mm FRP plate prestressed to 15%. Field applications, such as the Xinshuhe Bridge, have also demonstrated that prestressed CFRP plates can successfully address cracking problems and enhance durability when prestress levels of around 50% are applied [24]. In the shear domain, unbonded prestressed CFRP tendons combined with shear stirrups were found to enhance shear capacity by 56–78%, supporting truss–arch models [25], while externally bonded CFRP laminates were shown to partially restore flexural capacity in prestressed concrete girders experiencing strand loss [26].

Recent advancements (2024–2025) have significantly improved the understanding of prestressed CFRP plate applications for strengthening RC members. Wang et al. [27] proposed a novel bonded–unbonded externally prestressed CFRP system without end access, which can achieve better crack control and higher flexural capacity while reducing on-site installation constraints. Ayad et al. [28] developed a closed-form analytical model for interfacial stresses in simply supported RC beams reinforced with prestressed CFRP plates, explicitly considering the bending effects induced by prestressing and shear deformations in the adherends. Sharifi Ghalehnoei & Noormohammadi [29] performed finite element simulations showing that CFRP plate width and prestress level significantly affect ductility, failure mode, and load capacity, especially under realistic anchorage conditions. Lv et al. [30] used ABAQUS to investigate large-scale RC columns strengthened with prestressed CFRP sheets and concluded that prestressing significantly increases confinement efficiency. They also suggested strip wrapping with optimized confinement ratios, strip width, and spacing to achieve cost-effective improvements in load capacity and ductility. Chen et al. [31] proposed a circumferential prestressed CFRP method for large members and demonstrated that prestressing can improve confinement and delay the onset of failure. Gong et al. [32] tested gradually prestressed near-surface-mounted (NSM) CFRP strips and reported a reduced risk of debonding and improved flexural response compared with conventional NSM techniques.

Despite these extensive contributions, several critical gaps remain. Most experimental and numerical studies on prestressed CFRP-strengthened RC beams have focused on single-parameter optimization, such as prestress level, anchorage configuration, or plate layout, while limited attention has been given to the combined effects of CFRP plate width and prestress level on flexural performance, failure mechanisms, and serviceability parameters under realistic

mechanically anchored configurations [5–32]. Moreover, many reported anchorage systems are complex, proprietary, or expensive, and there is a lack of systematic comparative data on prestressed versus non-prestressed CFRP plates with variable widths using simple, locally adaptable mechanical anchorage systems suitable for resource-constrained practice. Furthermore, only a few studies explicitly relate experimental observations to capacity–demand ratios and design-oriented performance indicators, which are essential for transferring advanced prestressing concepts into practical guidelines for strengthening existing RC beams. These gaps hinder the development of rational and cost-effective design guidelines that relate CFRP plate geometry and prestress level to flexural capacity, ductility, and serviceability in a transparent and experimentally validated manner.

The novelty of this study is multifaceted and directly addresses these gaps. First, it presents a systematic experimental comparison of RC beams strengthened with variable-width prestressed and non-prestressed CFRP plates, thereby quantifying the coupled effects of plate geometry and prestress level on flexural response, ductility, cracking behavior, and failure mode, which have typically been investigated separately in previous studies. Second, it employs a practical and low-cost mechanical tensioning and anchorage system that can be constructed from locally available materials and installed without end access or specialized equipment, with the explicit goal of meeting the economic and logistical constraints common in developing countries. This approach directly addresses the lack of simple, field-adaptable anchorage systems reported in the literature. Third, the study includes experimentally derived capacity–demand ratios and serviceability indicators for various strengthening schemes, bridging the gap between detailed experimental behavior and design-oriented assessment while providing comparative benchmarks against recent prestressed CFRP developments [2, 27–32].

Accordingly, the main research question in this study is: How do CFRP plate width and prestress level (within the context of a practical mechanical anchorage system) interact to influence the flexural response, failure mode, and serviceability performance of RC beams compared with non-prestressed CFRP-strengthened and unstrengthened specimens?

To address this question, this paper presents an experimental study on RC beams strengthened with variable-width prestressed and non-prestressed CFRP plates using a mechanically anchored system suitable for practical implementation. The remainder of the paper is organized as follows. Section 2 describes the experimental program, including material properties, specimen design, strengthening schemes, and the test setup. Section 3 outlines the measurement procedures and data reduction methods. Section 4 presents and discusses the experimental results in terms of load–deflection behavior, cracking patterns, failure modes, and strain distribution. Section 5 compares the performance of prestressed and non-prestressed CFRP configurations, emphasizing the effects of plate width and prestress level and relating the results to existing literature. Finally, Section 6 summarizes the key conclusions and provides recommendations for design and future research.

2. Materials and Methods

Figure 1 provides a summary of the research methodology.

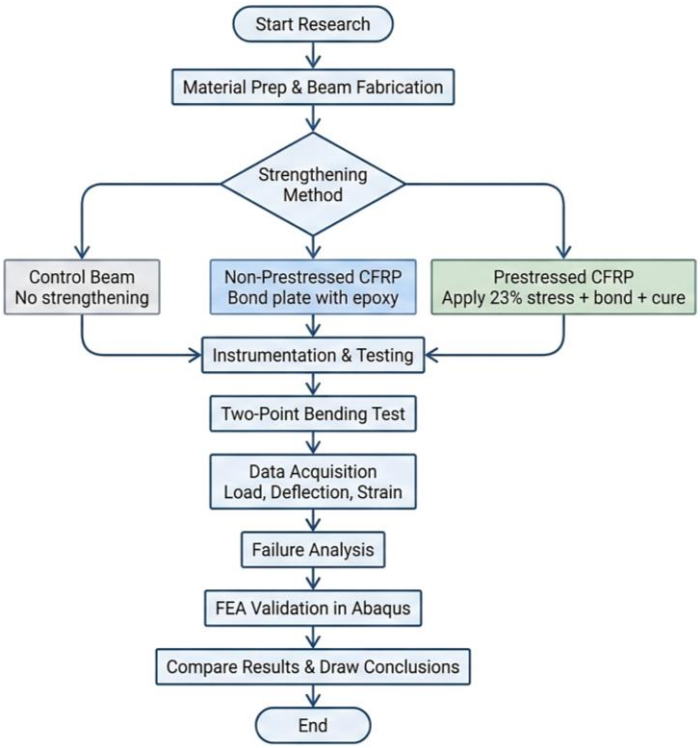

Figure 1. Research sequence flowchart

2.1. Theoretical Background

Prestressing externally bonded CFRP plates raises the position of the neutral axis, which decreases the strain gradient across the section and favors the uniform distribution of tensile stress in the CFRP. This mechanism enables a higher exploitation of the elastic range of the CFRP and postpones the occurrence of the localized debonding at critical interface zones. Accordingly, beams have improved deformability and load redistribution capability, which culminate in improved structural ductility and energy dissipation potential under both service and ultimate loading conditions [33-35]. Such ductility gains are of special interest in seismic-prone regions, where increased post-yield deformation capacity can lead to the slowing of brittle failure and higher collapse resistance.

The geometric configuration of the CFRP plate, in particular the width and thickness, has a decisive effect on the effectiveness of the stress transfer through the CFRP-concrete interface. Wider plates increase the bonded area and reduce the concentration of interfacial shear stress, which improves the anchorage efficiency and also enables a more even strain development in the FRP laminate [36, 37]. Nevertheless, excessive plate width relative to beam soffit dimensions may contribute to the problem of peeling stresses at ends of plate members, which is why optimum sizing based on fracture mechanics criteria needs to be emphasized. Bond-slip models and nonlinear finite-element simulations agree with the fact that debonding resistance is greatly improved when plate geometry is optimized with respect to adhesive properties and substrate roughness [38].

The combination of mechanical anchorage such as FRP U-wraps, fasteners, or end plates with externally bonded CFRP plates provides a synergistic strengthening system with reduced premature debonding failures. Such hybridization increases the effective length of anchorage and gives a confinement at termination zones, which helps in the full development of CFRP tensile forces [39-41]. Experimental investigations confirm that delayed interface-crack initiation and higher loads with more stable post-peak behavior are obtained for beams with such systems. Analytical formulations using models of fracture energy and cohesive zones further verify the effectiveness of mechanical anchorage in promoting ductile failure mechanisms in FRP-strengthened reinforced concrete members.

2.2. Material and Beam Design

The test program involved the investigation of the flexural behavior of externally bonded CFRP plates on RC beams in prestressed and non-prestressed states. To make a trustworthy comparison, each beam was cast with identical geometry, reinforcement, and material specifications. Concrete, reinforcing steel bars, and CFRP laminates were all used according to relevant structural standards. Each beam had a 2000 mm span, 300 mm depth (effective depth d = 242 mm), and 220 mm web thickness. The tension and compression faces were reinforced by 2*O16 deformed bars (16 mm diameter). Adequate shear resistance was obtained with O10, two-legged stirrups at 100 mm spacing, which ensured flexural failure. CFRP plates were bonded externally using a controlled prestress level or without a controlled prestress level to systematically observe the effect of this variable on flexural strength and failure modes. All plates were 1.4 mm thick and were available in three widths - 25 mm, 40 mm, and 60 mm. These widths were chosen to represent a practical, systematic range for flexural strengthening. The 25 mm width is a minimally invasive solution; the 60 mm width is a relatively wide plate, which is not impossible for external bonding and anchorage installation. The intermediate 40 mm width represents the transition between these extremes. All selected widths are compatible with locally available CFRP products and anchorage detailing in order for the experimental program to be of practical relevance.

Table 1. Details of test specimens

Beam ID	Strengthening Scheme	CFRP Plate Width (mm)	ρ_{cf} (Percentage of CFRP in The Beam)
RB	Control (un-strengthened)	–	-
RBCFB1	Non-prestressed, externally bonded	60	0.0015777
RBCFB2	Non-prestressed, externally bonded	40	0.0010518
RBCFB3	Non-prestressed, externally bonded	25	0.0006574
RBPCFB1	Prestressed, externally bonded	60	0.0015777
RBPCFB2	Prestressed, externally bonded	40	0.0010518
RBPCFB3	Prestressed, externally bonded	25	0.0006574

Table 2. Summary of test specimens' geometry and reinforcement details

Parameter	Value / Detail
Beam Length (L)	2000 mm (2.0 m)
Beam Height (H)	300 mm (30 cm)
Beam Effective Depth (d)	242mm (24.2cm)
Web/Thickness (t)	220 mm (22 cm)
Longitudinal Reinforcement	2Ø16 (top), 2Ø16 (bottom)
Shear Reinforcement	2-legged Ø10 stirrups @ 100 mm spacing

2.2.1. Concrete

The concrete used for the reinforced concrete beam specimens was designed to achieve a compressive strength of 23 MPa, as determined by cube tests after 23 days, in compliance with the requirements for flexural members. The mix design consisted of Ordinary Portland Cement (OPC) Type I, natural river sand from Al-Ukhaidir, Baghdad, and crushed limestone aggregate with a maximum size of 20 mm obtained from local quarries in Baghdad, representing the prevailing construction practices in the region. OPC Type I (IQS No. 5/1984) was used as the primary binder. It was supplied in 50 kg bags and stored under dry conditions to prevent premature hydration. The fine aggregate consisted of clean, well-graded siliceous sand from Al-Ukhaidir, which was washed and screened to achieve a fineness modulus of 2.6, making it suitable for structural concrete applications. The coarse aggregate consisted of locally available crushed limestone gravel with a maximum size of 20 mm and angular particles to ensure good interlocking and bonding characteristics. All aggregates were washed and kept in dry condition before use.

Table 3 presents a summary of the compressive strength, tensile strength, and modulus of elasticity of the concrete determined according to ASTM C39, ASTM C496-04, and ASTM C469, respectively. The measured slump of the mix was 75 mm. Table 4 shows the weight of each component of the concrete mix with a water–cement ratio of 0.45. The measured compressive strength of approximately 23 MPa corresponds to the strength level commonly found in existing reinforced concrete structures, particularly those constructed with conventional materials and without high-strength concrete requirements. This strength range is typical of normal building construction and infrastructure in many developing regions, as well as in older structures where strengthening and rehabilitation interventions are most frequently required. Therefore, the selected concrete strength provides a realistic basis for evaluating the effectiveness of CFRP strengthening systems under practical conditions rather than under optimized or high-performance concrete scenarios. At the same time, the use of moderate concrete strength allows the influence of CFRP strengthening and prestressing on flexural behavior and failure mechanisms to be clearly observed.

Table 3. Properties of concrete

Compressive strength (fc') MPa	Tensile strength (fct) MPa	Modulus of elasticity (Ec) MPa
23	2.68	22,540

Table 4. Mix design of concrete

Cement (kg/m^3)	Sand (kg/m^3)	Gravel (kg/m^3)
330	650	1,050

Figures 2 and 3 provide illustration of granulation diagrams for aggregate.

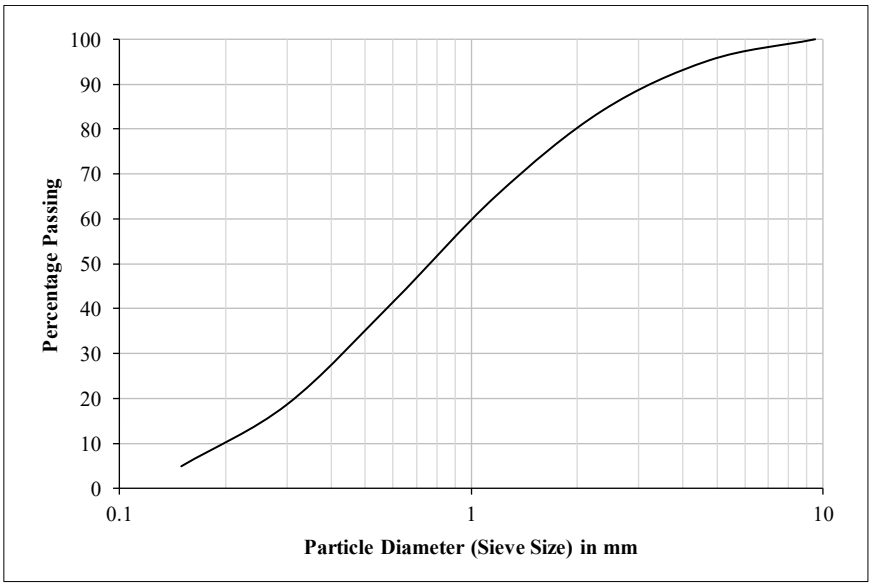

Figure 2. Granulation Diagram of Fine Aggregate

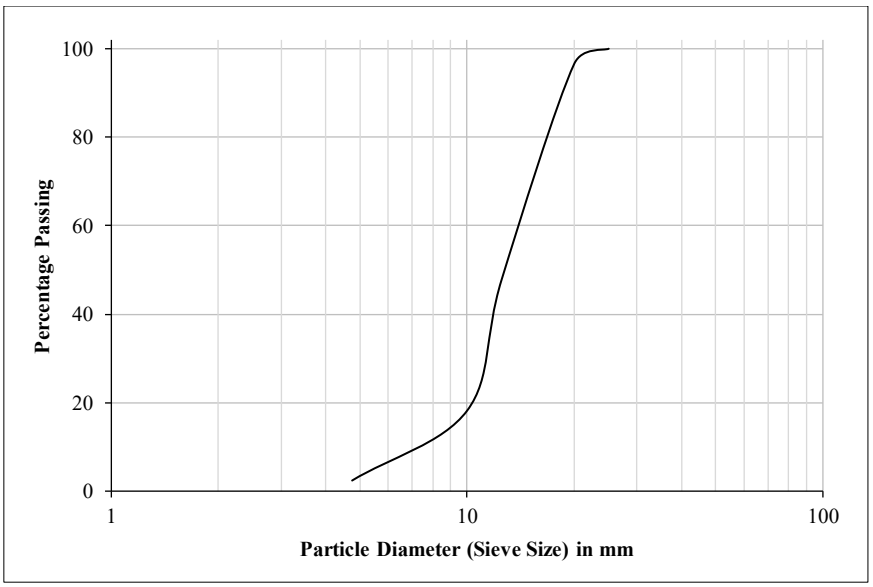

Figure 3. Granulation Diagram of Coarse Aggregate

2.2.2. Reinforcement Steel

The reinforcing steel used in the reinforced concrete beams was locally available and consisted of hot-rolled deformed bars of nominal diameters 10 mm and 16 mm. Tensile testing was performed to determine the mechanical properties, which met the structural requirements for flexural members and were in accordance with ASTM A370. The results are shown in Table 5.

Table 5. Test results and properties of reinforcement steel bars

Bar Diameter (mm)	Measured Yield Strength (*fy*) (MPa)	Measured Ultimate Strength (*fu*) (MPa)	Maximum Elongation (%)	Modulus of Elasticity (Es) (GPa)
10	440	612	14	200
16	460	644	13.2	200

2.2.3. Carbon Fiber Reinforced Polymer

Unidirectional CFRP laminates (Colmef HM-4T) were used to reinforce the reinforced concrete beams by applying the externally bonded technique with an epoxy adhesive along the tensile face. These aerospace-grade carbon fiber laminates are designed for structural strengthening applications and provide a high level of performance suitable for demanding engineering conditions. They exhibit strong resistance to chemicals, high temperatures (above 150 °C), cyclic loading, and seismically induced forces, indicating their potential suitability as retrofitting materials. The mechanical and physical properties are summarized in Table 6, while the CFRP plates used in this investigation are shown in Figure 4.

Table 6. Mechanical and Physical Properties of CFRP Laminates

Property	Value	Test/Condition
Appearance	Black, unidirectional laminate	–
Thickness	1.4 mm	Nominal
Width	100 mm (customizable)	Roll length: 100 m
Tensile Strength (Mean)	3100 MPa	Manufacturer data
Tensile Strength (Design)	2600 MPa	Manufacturer data
Elastic Modulus (Mean)	165,000 MPa	Manufacturer data
Elongation at Failure	1.70 %	–
Interlaminar Shear Strength	50 MPa	–
Bond Strength to Concrete	≥ 2.5 MPa (cohesive failure)	Pull-off test
Fiber Volume Content	≥ 65 %	–
Density	1.6 g/cm³	–
Temperature Resistance	> 150 °C	–
Shelf Life	50 years	Manufacturer specification

2.2.4. Adhesive Material

The carbon fiber reinforced polymer (CFRP) laminates were adhesively bonded to the concrete soffit using HM-120CP, a two-component structural epoxy with a weight ratio of A:B = 2:1. This adhesive offers great bond and shear strength, permits sag-free application in an overhead environment, and offers durable performance in aggressive environmental conditions. Full curing is achieved in 24 hours at ambient temperature, and the material exhibits excellent resistance to aqueous exposure, chemical agents, freeze/thaw cycling, fatigue, creep, and thermal aging. The principal mechanical characteristics are listed in Table 7.

Figure 4. The CFRP plates employed to strengthen the RC beam in this study

Table 7. Mechanical and durability properties of HM-120CP adhesive

Property	Value
Tensile strength (MPa)	62
Compressive strength (MPa)	117
Flexural strength (MPa)	115
Bond strength to concrete (MPa)	31
Fatigue resistance	2 × 10^6 cycles (no failure)
Partial curing time (min)	40–180
Full curing time	24 h
Resistance	Water, alkali, salts, acids, freeze–thaw, creep, thermal aging

2.3. Prestressing Method

The effect of active strengthening was then investigated through retrofitted CFRP prestressing. Prestressing was applied to the CFRP plates just before bonding, using a custom-built mechanical device that allowed the application and maintenance of a controlled level of tensile force during the epoxy curing process. The prestress intensity was 23% of the ultimate tensile strength of the CFRP material. Figure 5 shows the complete operation of the prestressing procedure.

Figure 5. Prestressing the CFRP plate which is sandwiched between the two steel anchorage plates

The prestress level applied to the CFRP plates was 23% of the ultimate tensile strength. This value was selected because it provides a significant prestressing effect while maintaining an adequate safety margin. It helps prevent premature debonding, overstressing of the anchorage system, and brittle failures at the CFRP–concrete interface.

Previous experimental studies have reported a wide range of prestress values. Lower prestress levels are generally used to control cracking and improve serviceability, whereas higher prestress levels can increase structural capacity but may introduce constructability challenges and anchorage-related problems.

In this investigation, only one prestress level was intentionally used in order to isolate the effect of CFRP plate width on the structural response, while keeping the prestressing parameter constant. The selected magnitude represents a moderate prestress level that can be easily achieved with the mechanical anchorage system used and allows stable force transmission during the loading sequence. The choice was also influenced by the availability of anchorage hardware and the use of locally available loading and prestressing equipment. Higher prestress magnitudes were not considered within the scope of this experiment to avoid introducing additional failure modes and to maintain consistency among all specimens.

2.3.1. Anchorage Devices

The end anchorage of the CFRP plates was implemented using a double-plate sandwich system to maximize the mechanical clamping force and prevent brittle peel-off failure. The main steel plate (detailed below) was first placed against the concrete surface of the RC beam. The CFRP plate was then positioned over this main plate. Subsequently, a secondary steel cover plate, identical or slightly smaller in size, was placed over the CFRP plate, thereby sandwiching the composite material between the two steel plates. High-strength bolts passing through both steel plates and either chemically anchored into the concrete beam or extending through the beam web were tightened to a specified torque. This process generated a high frictional clamping force on the CFRP surface along with direct shear resistance provided by the dense bolt pattern.

The use of slotted holes in the plates was necessary to allow the entire anchorage system to accommodate longitudinal strain (such as creep and shrinkage) without inducing excessive localized stresses in the composite material or concrete. An illustration of the steel anchorage plates and their configuration is shown in Figure 6, while Table 8 provides details of the plate geometry.

During installation of the mechanical anchorage system, the bolts were tightened using a calibrated torque wrench to ensure uniform torque application across all specimens. The same torque value was applied to all anchorage bolts to maintain consistency in clamping force and anchorage performance. Direct measurement of bolt slip was not performed during testing. However, anchorage performance was monitored indirectly through visual inspection, crack development, and load–deflection response. No premature end debonding or anchorage slippage was observed before failure in the prestressed specimens, indicating stable force transfer throughout the loading process. The effectiveness of the anchorage system was further confirmed by the rupture-controlled failure mode of the CFRP plates observed in all prestressed beams.

Table 8. Geometry of steel anchorage

Feature	Dimension (mm)	Role in Sandwich System
Overall Dimensions	450 × 320	This design provides sufficient surface area for a distributed clamping force
Circular Hole Diameter	18	This product accommodates high-strength bolts for clamping and shear transfer
Slotted Opening	200 × 18	This design allows for differential movement and strain accommodation of the RC beam
Longitudinal Pitch	80	Ensures a uniform distribution of bolt shear capacity
Transverse Pitch	Varies (50 to 105)	This statement dictates the width of the clamping zone across the CFRP plate
Plates Required	per anchorage end	Form the sandwich assembly around the CFRP plate

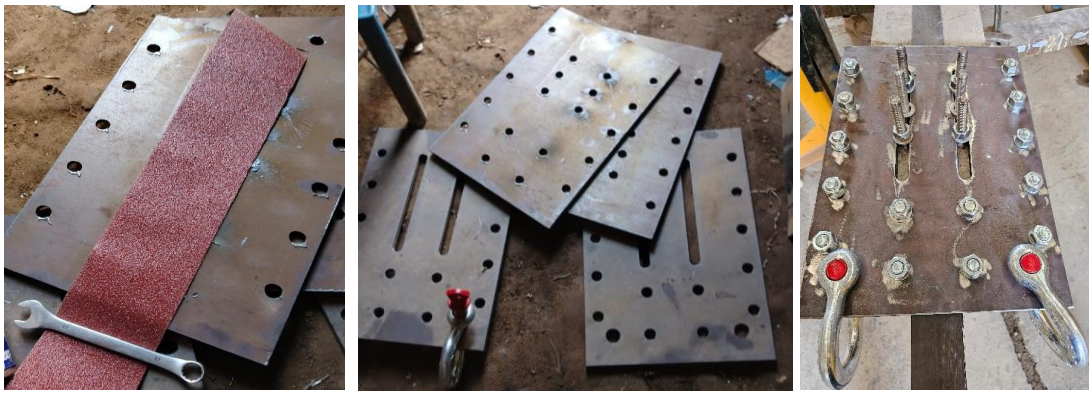

Figure 6. Images of the steel anchorage plates

2.3.2. Load Application System

Prestress was applied using a TOYO lever block (9-ton load capacity, 3 m lift, grade T-10 mm chain), as specified in the inspection certificate. Together with a heavy-duty shackle and steel chain, the lever hoist allowed slow and controlled loading of the CFRP plates. This setup made it possible to adjust the prestressing step by step in a secure and stable manner.

2.3.3. Testing Frame and Support

The entire system was secured within a rigid steel loading frame to prevent misalignment or eccentric stresses. The frame allowed the CFRP laminates to be stretched along the soffit of the RC beam and helped maintain the applied prestress uniformly along the bonded length. All these details are illustrated in Figure 7.

2.3.4. Instrumentation and Control

The prestressing force was measured using an online electronic load cell (see also Figure 7). This ensured that the target prestress level was accurately achieved and maintained during the bonding process. The use of calibrated measuring instruments minimized errors in the stress levels applied to the specimens.

2.3.5. Bonding Under Prestress

After the CFRP plate was stressed to the target value, a layer of epoxy adhesive (HM-120CP) was applied at the interface between the CFRP plate and the beam surface. The laminates were then pressed onto the pre-prepared soffit of the beam. The applied prestress was maintained during the curing period of the adhesive (at least 24 hours), allowing the CFRP to be activated from the moment load was applied. This process delayed the onset of damage in the strengthened beams.

This prestressing procedure enabled the simulation of field-strengthening techniques in a controlled and practical laboratory environment while maintaining operator safety and load accuracy. Details of the equipment—including the anchorage system, lever block, shackles, chains, and the overall test frame—are shown in Figure 7.

2.4. Experimental Setup

Static flexural loading was used to investigate the structural behavior of the reinforced concrete beams for both the control specimens and the CFRP-strengthened cases. A custom test rig was designed to provide realistic structural loading conditions, capture failure modes, and obtain reproducible experimental data for validation purposes. The following sections describe in detail the loading frame, loading types and support conditions, instrumentation, and testing procedures.

2.4.1. Test Frame and Loading Capacity

All specimens were tested within a rigid steel reaction frame capable of resisting high static forces without significant self-deformation. The frame was designed for a maximum capacity of 500 kN, providing an adequate safety margin relative to the expected ultimate loads of the tested beams.

The load was applied using a hydraulic jack acting on a steel spreader beam positioned above the specimen. The spreader beam distributed the load into two symmetrically connected loading points along the beam. This arrangement ensured uniform load transfer while minimizing eccentricity and local crushing effects. The entire system was firmly anchored to the laboratory strong floor to prevent vibration or lateral movement during testing. Prior to each test, the alignment and rigidity of the frame system were visually inspected to ensure proper operation.

2.4.2. Loading Arrangement and Support Conditions

The control beams were tested using a two-point bending configuration, which produced a constant bending moment in the central span while allowing shear effects to develop near the supports. This configuration was selected to impose the maximum possible flexural demand on the specimens and to directly evaluate the effectiveness of CFRP strengthening.

The beams were supported on steel roller supports, providing a simply supported boundary condition and allowing free rotation and horizontal movement. This arrangement simulated idealized structural boundary conditions and minimized restraint forces that could influence the bending behavior. The resulting loading diagram is shown in Figure 7, while Table 9 summarizes the main geometric parameters of the loading configuration.

Table 9. Loading Arrangement and Support Details

Parameter	Value	Description
Loading method	Two-point static loading	Hydraulic jack with spreader beam
Apparatus load capacity	500 kN	Steel reaction frame
Beam total length	2000 mm	Including support regions
Clear span	1600 mm	Between roller supports
Bearing length	200 mm (each end)	Contact zone at supports
Distance between load points	320 mm	Center-to-center spacing
Distance from supports to load pts	640 mm	Equal spacing both sides
Boundary condition	Supported (rollers)	Rotation and translation permitted

Figure 7. Test setup

2.5. Instrumentation

An instrumentation system was developed to measure load, deflections, concrete strains, steel reinforcement strains, and CFRP strains throughout the loading history. A combination of electronic strain gauges, displacement transducers, and load monitoring devices was used.

2.5.1. Deflection Measurement

Deflections were measured using linear variable displacement transducers (LVDTs) with a resolution of ±0.01 mm. For each specimen, three LVDTs were employed: one positioned at the mid-span, corresponding to the point of maximum deflection, and two others placed symmetrically at the quarter-span positions to monitor beam curvature and support rotations. The transducers were mounted on independent supports to minimize external interference and were isolated from the test frame. Figure 8 shows the LVDT setup used in the test.

Before testing began, all LVDTs and strain gauges were calibrated according to the manufacturer's specifications and standard laboratory procedures. The LVDTs used at the mid-span have a typical accuracy of ±1% of full scale, while the electrical resistance strain gauges have an expected accuracy of approximately ±1–2% under controlled laboratory conditions.

Considering the magnitude of the measured deflections, strains, and load increments during the experimental program, the expected measurement uncertainties are negligible compared with the overall response trends and therefore do not affect the interpretation of the experimental results.

Figure 8. LVDTs under tested beam

2.5.2. Load Measurement

The applied load was continuously monitored using a calibrated load cell placed directly beneath the hydraulic jack. The load cell was connected to the data acquisition (DAQ) system, ensuring synchronization with the strain and deflection measurements.

2.5.3. Crack Monitoring

Flexural and shear cracks were observed visually and marked on the beam surfaces using a fine-tip marker at each load increment. Crack widths were measured at selected stages using a crack comparator microscope. Photographic documentation was also performed throughout the testing process.

2.6. Data Acquisition System

All strain gauges, LVDTs, and the load cell were connected to a computerized data acquisition system (DAQ) capable of recording multi-channel signals at a sampling rate of 5 Hz. The DAQ system enabled real-time display and storage of load–deflection–strain curves, providing synchronized datasets for post-processing and analysis. Calibration checks were performed before each test. Figure 9 shows the DAQ system in operation.

Figure 9. Data Acquisition System and all connected devices

3. Testing Procedure

The detailed test procedures for four groups of reinforced concrete (RC) beams subjected to static, monotonic, two-point flexural loading are presented in this section. The loading progression was identical for all beam types and was conducted under controlled laboratory conditions. The tests aimed to investigate the maximum flexural behavior, crack propagation, and ultimate failure modes of the beams strengthened with bonded or prestressed CFRP plates. The categories and testing procedures of the beams are described as follows.

3.1. The First Procedure: Control Beams

One control beam was used as a benchmark against which all CFRP-strengthened configurations were compared. The specimen was mounted on roller supports with a clear span of 1,600 mm. Strain gauges were installed on both the steel reinforcement and the concrete surface. In addition, LVDTs for load–deflection measurements and load cells for monitoring the applied load were installed and calibrated prior to testing.

The load was applied incrementally using a two-point bending system. The load was gradually increased until failure, while crack development, deflection, and strain responses were continuously monitored. At each load increment, a visual crack map was recorded.

3.2. The Second Procedure: Beams Strengthened with Externally-Bonded Non-Prestressed CFRP Plates

In this investigation, three beam specimens were strengthened by applying externally bonded CFRP plates to the tension face of the soffit. The strengthening procedure was completed 24 hours before testing. Surface preparation included mechanical grinding of the concrete soffit followed by cleaning with compressed air to maximize adhesion. The CFRP plates were lightly abraded with sand and then cleaned with acetone.

Both the concrete surface and the CFRP plates were coated with a two-component structural epoxy adhesive (HM-120CP). The laminates were then pressed against the prepared beam surface and held in place to ensure proper contact. The bonded system was allowed to cure for at least 24 hours at ambient temperature.

On the testing day, each strengthened beam was placed on the test rig using the same support conditions as the unreinforced control beam. Standardized procedures were followed for all specimens. The load was increased at a controlled rate until failure while data were recorded continuously throughout the loading sequence. Particular attention was given to the onset of cracking, interfacial bond behavior, and any signs of CFRP debonding. The three specimens were reinforced with CFRP plates of different widths (25 mm, 40 mm, and 60 mm).

3.3. The Third Procedure: Beams Strengthened with Externally Bonded Prestressed CFRP Plates

This strengthening approach represents the most advanced reinforcement technique used in this study, combining composite action with external prestressing. The procedure involved three beams, requiring precise coordination between surface preparation, prestressing, and adhesive application. The soffit of each beam and the CFRP plates were cleaned and then roughened through abrasive treatment in accordance with the specified bonding protocol.

A prestressing apparatus was used to apply predetermined strains to the CFRP laminates using a mechanical prestressing frame consisting of a lever block and load-cell system. The prestressed CFRP plates were then bonded to the beam surface using epoxy adhesive while maintaining the applied prestress. The plates remained tensioned for more than 24 hours, allowing the adhesive to cure under prestress and enabling early activation of the CFRP during the flexural response.

After curing, the beam was transferred to the instrumented loading frame. Once the adhesive curing process was complete, the prestressing device was released, while the prestress remained locked within the bonded CFRP laminate. The loading protocol was monotonic and unidirectional, applied at a constant loading rate, while all structural responses were continuously monitored. Failure was defined as rupture of the CFRP laminate, bond failure at the CFRP–concrete interface, or flexural failure of the beam. Consistent with the strengthening configuration, variations in CFRP plate width produced the expected differences in structural behavior.

4. Results

4.1. Control Beam

As shown in Figure 10, the control beam (RB) was tested under a two-point bending configuration to evaluate its flexural behavior without any strengthening measures. The specimen exhibited the expected progression of flexural damage, beginning with the appearance of fine tensile cracks at the mid-span region. These cracks gradually propagated and widened as the applied load increased. With further load increments, the cracks extended vertically and diagonally toward the compression zone, which is typical of flexural–shear interaction development.

The primary flexural crack initiated at mid-span, where the bending moment reached its maximum value, leading to significant concrete crushing and large deflection. The crack pattern on the beam surface consisted of a central longitudinal crack accompanied by several secondary cracks distributed symmetrically on both sides, which corresponds

to the classical failure pattern of reinforced concrete members subjected to bending. Accordingly, the overall failure mode of the control beam can be classified as flexural failure, characterized by yielding of the tensile reinforcement followed by crushing of the concrete in the compression zone. This behavior is consistent with the expected response of an unstrengthened reinforced concrete beam under monotonic loading.

The load–displacement relationship is a critical parameter in structural testing because it provides a comprehensive representation of the mechanical response of a beam throughout the entire loading process. While visual inspection and crack patterns reveal the failure mechanism, the load–displacement curve quantitatively describes the relationship between the applied load and the corresponding deflection (or displacement) at key locations, typically at the mid-span for flexural members. Figure 11 presents the experimental load–displacement curve obtained for the control specimen.

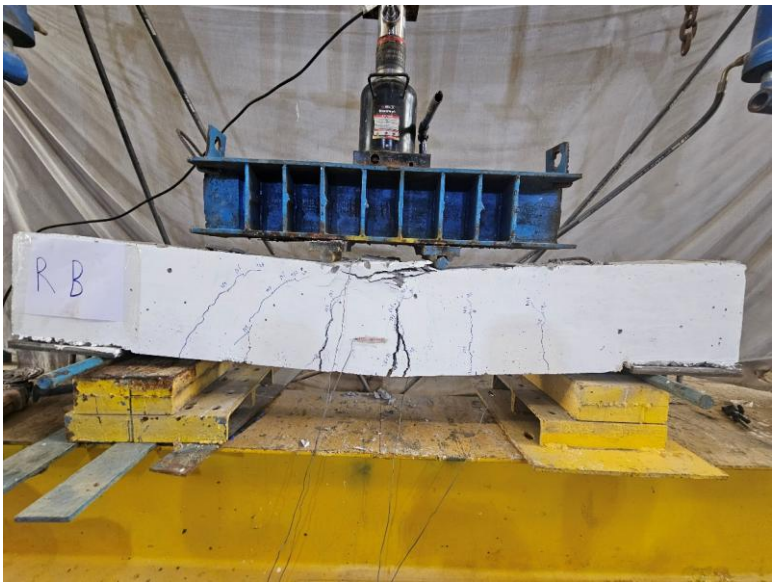

Figure 10. Control beam (RB) after loading

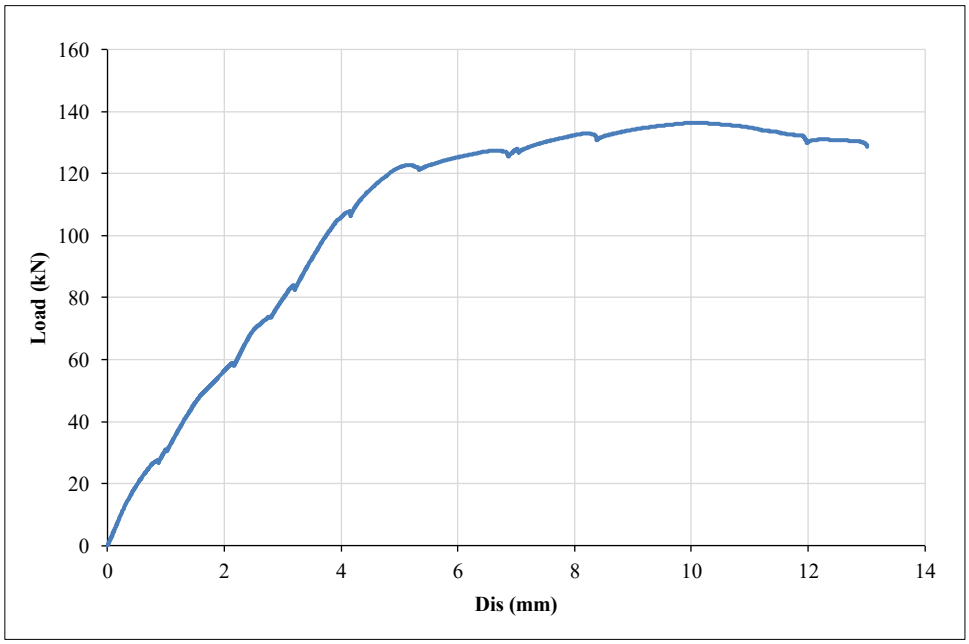

Figure 11. Load-Displacement curve for control (RB) beam

4.2. Externally-Bonded Non-Prestressed CFRP-Strengthened Beams

Figures 12, 13, and 14 illustrate the strengthened beams with CFRP plates of different widths: 60 mm (RBCFB1), 40 mm (RBCFB2), and 25 mm (RBCFB3), respectively. The corresponding load–displacement curves are presented in Figure 15.

Figure 12. RC Beam strengthened with a 60mm CFRP plate, after loading

Figure 13. RC Beam strengthened with a 40mm CFRP plate, after loading

Figure 14. RC Beam strengthened with a 25mm CFRP plate, after loading

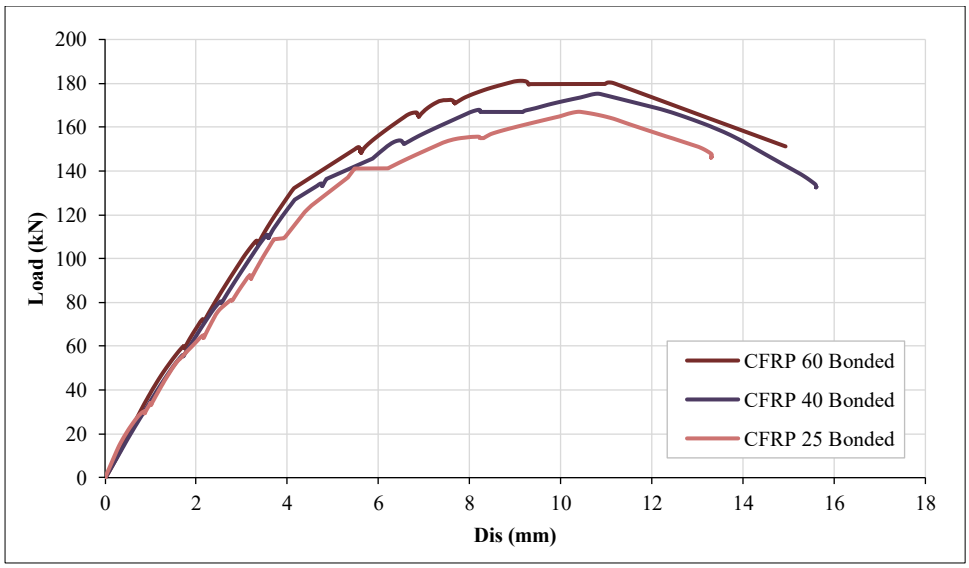

Figure 15. Load-Displacement curve for strengthened (RBCFB1, RBCFB2 & RBCFB3) beams

4.3. Externally-Bonded CFRP-Strengthened Beams

Figures 16, 17, and 18 represent the strengthened beams with different widths of the prestressed CFRP plate: 60 mm (RBPCFB1), 40 mm (RBPCFB2), and 25 mm (RBPCFB3), respectively, while Figure 19 shows the load-displacement curve.

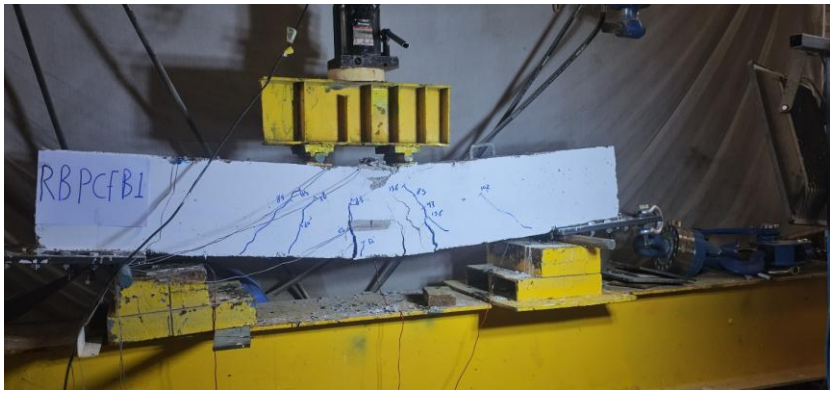

Figure 16. RC Beam strengthened with a 60mm prestressed CFRP plate, after loading

Figure 17. RC Beam strengthened with a 40mm prestressed CFRP plate, after loading

Figure 18. RC Beam strengthened with a 25mm prestressed CFRP plate, after loading

The three beams—RBPCFB1 (60 mm CFRP), RBPCFB2 (40 mm CFRP), and RBPCFB3 (25 mm CFRP)—were strengthened with prestressed CFRP plates and subjected to a prestress equal to 23% of their ultimate tensile capacity. All specimens ultimately failed due to rupture of the CFRP plates. The application of prestressing had a significant influence on the cracking behavior and the overall flexural response compared with the non-prestressed members.

In the RBPCFB3 beam (25 mm plate), cracking was uniformly distributed along the span, and the crack widths remained relatively small, indicating that the prestress effectively delayed the appearance of visible cracks and improved serviceability. Failure occurred by CFRP rupture at mid-span following progressive flexural cracking, demonstrating the full utilization of the CFRP reinforcement.

In the RBPCFB2 beam (40 mm plate), fewer cracks were observed, and they were mainly concentrated near the mid-span region. The applied prestress allowed the beam to sustain higher loads with smaller deflections compared with its non-prestressed counterpart. The CFRP plate ruptured near the location of maximum bending moment, and localized crushing of the concrete in the compression zone occurred, indicating efficient stress transfer between the CFRP and the concrete substrate.

The RBPCFB1 beam (60 mm plate) exhibited the highest load-carrying capacity among the specimens. The cracks were fewer in number but steeper, suggesting that prestressing further enhanced flexural resistance and delayed crack initiation. However, failure occurred abruptly and in a brittle manner due to CFRP rupture, accompanied by severe crushing in the compression zone. This behavior confirms that the full tensile capacity of the CFRP was reached before any debonding occurred.

Overall, all three prestressed CFRP-strengthened beams failed due to rupture of the CFRP plates, confirming the presence of a strong bond and effective utilization of the strengthening system. Prestressing improved cracking performance, increased load-carrying capacity, and reduced deflections, particularly for the beams with wider CFRP plates. However, as the width of the CFRP plate increased, the failure mode became more brittle, highlighting the importance of carefully optimizing the plate width and prestress level to achieve a balance between strength and ductility.

4.4. Comparison of Ultimate Load and Deflection Enhancement

The maximum load and mid-span deflection at failure for all specimens were measured to evaluate the effectiveness of both prestressed and non-prestressed CFRP strengthening systems. These results are presented in Table 10, where the flexural capacity of the strengthened beams is compared with that of the control specimen (RB). The increase in load-carrying capacity is expressed as a percentage of the ultimate load, highlighting the influence of CFRP plate width and prestressing on the overall structural performance. The load–displacement responses of the specimens are illustrated in Figure 19.

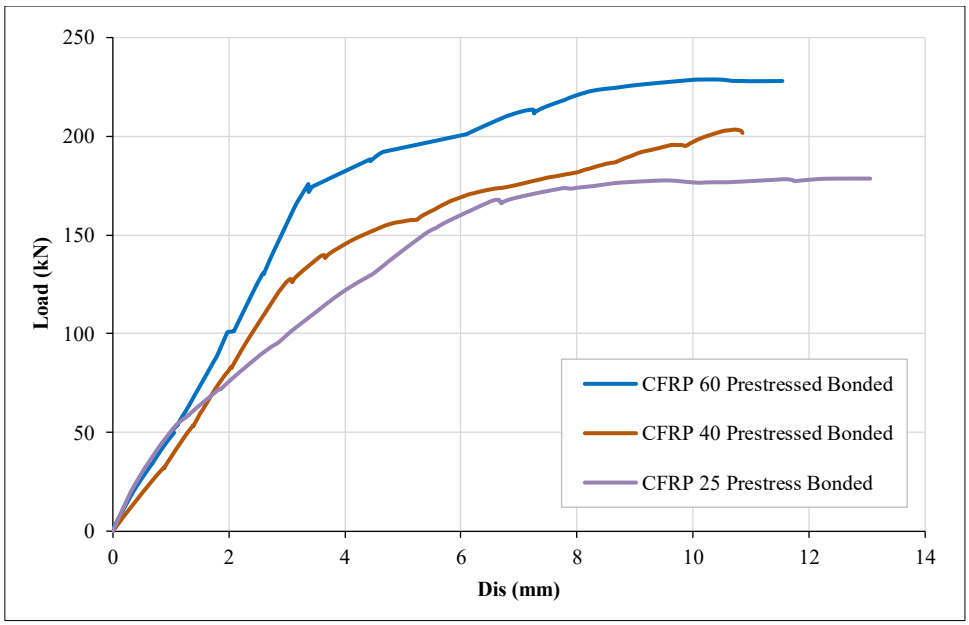

Figure 19. Load-Displacement curve for prestressed CFRP-strengthened (RBPCFB1, RBPCFB2 & RBPCFB3) beams

Table 10. Ultimate load & corresponding mid-span deflection of tested beams, and percentage enhancement relative to control beam (RB)

Beam ID	Strengthening Type	CFRP Plate Width (mm)	Ultimate Load (kN)	Mid-Span Deflection at Ultimate Load (mm)	Load Enhancement Percentage (%)
RB	Control (Un-strengthened)	–	136.35	10.10	–
RBCFB3	Non-prestressed CFRP	25	166.91	10.34	22.4
RBCFB2	Non-prestressed CFRP	40	175.27	10.79	28.5
RBCFB1	Non-prestressed CFRP	60	180.42	11.06	32.3
RBPCFB3	Prestressed CFRP	25	176.95	10.80	29.8
RBPCFB2	Prestressed CFRP	40	203.30	10.73	49.1
RBPCFB1	Prestressed CFRP	60	228.55	10.66	67.6

5. Discussion

5.1. Load-Deflection Behavior

Load–deflection data indicate that externally bonded CFRP plates, both non-prestressed and prestressed, significantly enhanced the flexural performance of the tested reinforced concrete beams compared with the unstrengthened control specimen (RB). The control beam reached an ultimate load of 136.35 kN with a mid-span deflection of 10.10 mm. In the non-prestressed CFRP series (RBCFB), increasing the plate width from 25 mm to 60 mm resulted in a systematic increase in ultimate load from 166.91 kN (RBCFB3) to 175.27 kN (RBCFB2) and 180.42 kN (RBCFB1). Correspondingly, the mid-span deflections at ultimate load were 10.34 mm, 10.79 mm, and 11.06 mm, respectively. These results suggest that increasing the plate width improved structural capacity, while the ultimate deflections remained similar to those of the control beam, indicating enhanced strength without a significant increase in deformation demand at failure.

The prestressed CFRP series (RBPCFB) showed further increases in load capacity compared with the non-prestressed strengthening with equivalent plate widths. The ultimate loads increased to 176.95 kN, 203.30 kN, and 228.55 kN for plate widths of 25 mm, 40 mm, and 60 mm, corresponding to specimens RBPCFB3, RBPCFB2, and RBPCFB1, respectively. Importantly, the mid-span deflections at ultimate load remained within a narrow range—10.80 mm, 10.73 mm, and 10.66 mm, respectively—remaining comparable to those of the control and non-prestressed specimens despite the higher load capacities.

The load–displacement curves shown in Figures 15 and 19 support these observations by illustrating the comparative response of the non-prestressed and prestressed strengthened beams and highlighting the influence of plate width and prestressing on the overall structural response. Within the prestressed group, the results further indicate that prestressing provides higher load resistance with smaller deflections compared with the corresponding non-prestressed beams, which is consistent with the observed curve behavior and ultimate-state measurements.

5.2. Cracking Behavior and Serviceability Response

The cracking behavior observed in the control specimen (RB) provides the baseline serviceability response for the unstrengthened beam. Under monotonic two-point bending, RB exhibited the typical progression of flexural cracking: fine tensile cracks initially appeared at the mid-span region and subsequently propagated and widened as the applied load increased. With continued loading, the cracks extended vertically and developed diagonal components toward the compression zone, indicating the interaction between flexure and shear as failure approached. The final crack pattern was dominated by a primary flexural crack at mid-span accompanied by several secondary cracks distributed symmetrically along the span, resulting in flexural failure controlled by concrete crushing in the compression zone.

In the prestressed CFRP-strengthened beams (RBPCFB), a distinct change in cracking behavior was observed compared with both the control and the non-prestressed strengthened specimens. All prestressed beams were tensioned to 23% of the CFRP tensile capacity, which delayed crack initiation and improved crack control. In RBPCFB3 (25 mm CFRP width), cracks were uniformly distributed along the span and exhibited relatively small widths, indicating effective redistribution of tensile stresses and improved serviceability performance. As the CFRP plate width increased while maintaining the same prestressing level, cracking became more localized. RBPCFB2 (40 mm) exhibited fewer cracks concentrated near the mid-span, whereas RBPCFB1 (60 mm) showed even fewer but steeper cracks, consistent with increased flexural capacity and higher load resistance.

From a serviceability perspective, prestressing the CFRP plates improved resistance to crack initiation and maintained crack widths at relatively small levels while keeping the mid-span deflections at ultimate load within a narrow range for all specimens. Despite the significantly increased loads, the ultimate deflections of the prestressed beams remained comparable to those of the control and non-prestressed beams, indicating that strength enhancement was achieved without a corresponding increase in deformation demand.

In the non-prestressed CFRP-strengthened beams (RBCFB), cracking was accompanied by partial debonding and progressive concrete cracking prior to failure, indicating less effective control of tensile stresses at the concrete–CFRP interface compared with the prestressed configuration.

Crack development in all specimens was monitored throughout the tests using visual tracing and crack-width measurements, allowing a consistent comparison of the serviceability behavior among the tested beam groups.

5.3. Influence of CFRP Prestressing and Plate Width on Ultimate Capacity

The ultimate capacity results show that both CFRP plate width and prestressing significantly increased the flexural load resistance of the tested RC beams compared with the control specimen (RB). The control beam reached an ultimate load of 136.35 kN.

5.3.1. Effect of CFRP Plate Width Without Prestressing (RBCFB Series)

For the non-prestressed CFRP-strengthened beams (RBCFB), increasing the CFRP plate width from 25 mm to 60 mm resulted in a gradual increase in ultimate load. The ultimate load increased from 166.91 kN at a plate width of 25 mm, to 175.27 kN at 40 mm, and to 180.42 kN at 60 mm.

Correspondingly, the percentage increase in ultimate load rose from 22.4% at 25 mm, to 28.5% at 40 mm, and 32.3% at 60 mm. This trend confirms that increasing the width of the CFRP plate enhances its contribution to flexural strengthening, resulting in progressively greater ultimate load capacities.

5.3.2. Additional Influence of Prestressing at the Same Plate Widths (RBPCFB Series)

The introduction of prestressing at a level of 23% had a significant effect on the ultimate capacity for all plate widths. For the 25 mm plate, prestressing increased the ultimate load from 166.91 kN (non-prestressed) to 176.95 kN (prestressed), corresponding to a 29.8% increase compared with the reference beam (RB).

For the 40 mm plate, the ultimate load increased from 175.27 kN to 203.30 kN, resulting in an improvement of 49.1%. The largest increase was observed for the 60 mm plate, where prestressing increased the ultimate load from 180.42 kN to 228.55 kN, corresponding to a maximum enhancement of 67.6%.

Overall, the results demonstrate a clear interaction between CFRP plate width and prestressing, where increasing the plate width enhances the strengthening effect, and prestressing provides an additional capacity gain that becomes more significant as the plate width increases. This interaction is consistent with the observed flexural response, with the 60 mm prestressed configuration (RBPCFB1) exhibiting the highest load-carrying capacity among the tested specimens.

5.4. Failure Modes and Load Transfer Mechanisms

The observed failure modes highlight clear differences among the unstrengthened beam, the non-prestressed CFRP-strengthened beams, and the prestressed CFRP-strengthened beams, reflecting changes in stress transfer along the tension face and at the CFRP–concrete interface. The control beam (RB) exhibited a conventional flexural failure governed by reinforcement yielding and concrete crushing in the compression zone. This failure was preceded by progressive flexural cracking concentrated at mid-span, where the bending moment reaches its maximum value. This baseline response indicates that the internal steel reinforcement and concrete resisted the tensile–compressive force couple without the participation of external composite reinforcement.

For the non-prestressed CFRP-strengthened beams (RBCFB), the failure response involved partial debonding accompanied by progressive concrete cracking prior to failure. This behavior corresponds to an interface-controlled mechanism, in which increasing load demand progressively elevates interfacial stresses at the CFRP–concrete interface, eventually causing localized loss of composite action and limiting the ability to fully mobilize the tensile capacity of the CFRP reinforcement.

In contrast, all prestressed CFRP-strengthened beams (RBPCFB1–RBPCFB3) failed due to CFRP plate rupture, with rupture occurring at or near the mid-span, which corresponds to the critical section of maximum bending moment. In RBPCFB3 (25 mm), rupture occurred at mid-span following progressive flexural cracking, indicating effective engagement of the CFRP reinforcement up to failure. In RBPCFB2 (40 mm), CFRP rupture was accompanied by localized concrete crushing in the compression zone, demonstrating efficient stress transfer between the CFRP reinforcement and the concrete at high load levels. The RBPCFB1 specimen (60 mm) exhibited the most sudden and brittle response, with CFRP rupture accompanied by severe crushing of the concrete in the compression zone, confirming that rupture occurred before any premature debonding developed.

The transition from partial debonding in the non-prestressed configuration to CFRP rupture in the prestressed configuration indicates that the prestressed system provided a stronger and more reliable load transfer mechanism, enabling substantially higher utilization of the CFRP tensile capacity. This rupture-controlled behavior further confirms the effectiveness of the mechanical sandwich anchorage system in preventing premature end debonding and maintaining composite action up to peak load. At the same time, the more brittle rupture-dominated behavior observed in the wider prestressed configurations indicates a reduction in post-peak ductility as the CFRP contribution increases. This finding highlights the importance of balancing strength enhancement and deformation capacity when selecting CFRP plate width under a fixed prestress level.

5.5. Comparison with Previous Experimental Studies

The experimental results of the present investigation are consistent with, and in some aspects surpass, the findings of previous studies on the flexural strengthening of reinforced concrete (RC) beams using prestressed CFRP plates. In particular, improvements in crack control and ultimate moment capacity, especially at higher prestressing levels such as 23% prestress, demonstrate the effectiveness of the integrated mechanical anchorage system and the optimized configuration of CFRP plate width.

Experimental verification of the ductile response of prestressed CFRP-strengthened RC beams was reported by Yang et al. [42], who observed a 47% increase in ultimate load at prestress levels close to 30%. This improvement was primarily attributed to elastic–plastic end-anchorage development and strain redistribution. The present study demonstrates flexural performance comparable to, or better than, that reported by Yang et al., despite using a less complex mechanical anchorage configuration, thereby highlighting the effectiveness of the proposed sandwich anchorage system. Similarly, Badawi & Soudki [43] reported an enhancement of up to 62% in flexural strength for beams strengthened with prestressed near-surface-mounted CFRP rods; however, their method required extensive groove preparation and detailed anchorage provisions. In contrast, the present investigation achieves comparable improvements using surface-bonded CFRP plates, which facilitates constructability and reduces retrofit time.

Attari et al. [34] investigated the influence of CFRP plate width and concluded that wider plates lead to greater flexural capacity but also increase the risk of premature debonding in the absence of adequate anchorage. The results obtained in the present study confirm this observation. However, the mechanical anchorage system adopted here effectively suppressed debonding—even at the maximum plate widths—allowing full utilization of the CFRP tensile capacity. Furthermore, Hadi et al. [39] evaluated full-scale RC beams strengthened with different FRP configurations and found that the combination of prestressing and anchorage produced more ductile failure modes and reduced crack widths by up to 40%. These findings are consistent with the trends observed in the present study, particularly the transition from more brittle to more ductile response regimes when prestress levels exceed 15%.

Finally, fracture mechanics investigations by Slaitas et al. [37] demonstrated that bond–slip behavior governs the interface response in the absence of sufficient anchorage. In contrast, the experimental results of the present study show that the adopted anchorage strategy promotes cohesive failure within the concrete matrix, thereby eliminating premature interface debonding. This represents a significant improvement compared with non-anchored configurations.

Overall, many previous studies have focused on single parameters, such as prestress level, plate type, or bond characteristics. In contrast, the experimental program presented in this investigation provides a more comprehensive understanding of the synergistic interaction between prestress ratio and CFRP plate width. Consequently, the results offer valuable insights that can improve retrofit strategies for full-scale structural members.

Table 11 presents a comparative analysis of the flexural strengthening results obtained from prestressed CFRP systems in the present study alongside selected recent experimental studies. The table summarizes key parameters, including prestress level, CFRP plate width, anchorage strategy, and failure mode, to highlight performance trends and recent developments in this research field.

Table 11. Comparison with Previous Experimental Studies on Prestressed CFRP-Strengthened RC Beams

Study	Prestress Level	Max CFRP Plate Width	Ultimate Load Gain Over Control	Failure Mode	Anchorage Type	Main Contribution
Current Study (RBPCFB1)	23% CFRP capacity	60 mm	+67.6% (228.55 vs. 136.35 kN)	CFRP rupture + crushing (no debonding)	Mechanical sandwich anchors	Synergistic effect of width + prestress, no debonding
Yang et al. [42]	30% CFRP capacity	Not specified	~47%	CFRP rupture, ductile	Elastic-plastic end supports	Ductile behavior verification
Badawi & Soudki [43]	Up to 35% (NSM rods)	NSM rods	Up to 62%	CFRP rupture (anchored NSM)	Custom NSM groove anchors	NSM prestressing efficiency
Attari et al. [34]	None	Up to full soffit	~32%	Risk of debonding at large widths	Not emphasized	Width impact on strength
Hadi et al. [39]	Various (some prestressed)	Varies	~40–60%	Ductile, crack-controlled	Various mechanical types	Full-scale validation of serviceability
Slaitas et al. [37]	None	Varies	Not reported (focus on interface)	Debonding when unanchored	None or minimal	Fracture mechanics of interface

6. Conclusions

This study experimentally investigated the flexural response of reinforced concrete beams strengthened with externally bonded carbon fiber reinforced polymer (CFRP) plates, with particular emphasis on the combined influence of prestressing and plate width. The experimental results clearly demonstrate that CFRP strengthening is an effective technique for improving flexural capacity, stiffness (modulus of elasticity), and cracking behavior, while prestressing provides a significant contribution to performance enhancement. Compared with the unstrengthened reference beam, non-prestressed CFRP plates increased the ultimate load by 22.4% to 32.3% as the plate width increased from 25 mm to 60 mm. When a prestress level of 23% was applied, the ultimate load enhancement increased further to 29.8%, 49.1%, and 67.6% for plate widths of 25 mm, 40 mm, and 60 mm, respectively. Prestressing also improved serviceability performance by delaying crack initiation and limiting crack widths, while the mid-span deflections remained comparable to those of the non-prestressed specimens, despite the substantial increase in load-carrying capacity.

The delayed onset of cracking observed in the prestressed specimens confirms the theoretical role of prestressing in inducing compressive stresses in the concrete tension zone. Furthermore, the transition from premature debonding to higher load capacities demonstrates the effectiveness of the mechanical anchorage system in mobilizing the tensile strength of the CFRP plates, which is consistent with the fundamental principles of fiber-reinforced polymer strengthening.

Observations of the failure modes further confirm the effectiveness of the prestressed CFRP system. While the non-prestressed beams exhibited partial debonding and progressive concrete cracking prior to failure, all prestressed specimens failed by CFRP rupture at mid-span, indicating efficient stress transfer and full utilization of the composite reinforcement. This outcome validates the adequacy and reliability of the proposed mechanical sandwich anchorage system in preventing premature debonding. The results also indicate that flexural strength increases with increasing CFRP plate width, although this improvement tends to reduce post-peak ductility, particularly in prestressed configurations where failure becomes more brittle. Therefore, an optimized strengthening strategy should carefully balance the CFRP plate width and prestress level in order to achieve the desired strength while maintaining adequate ductility.

Overall, the results of this study provide experimental evidence supporting the use of prestressed CFRP plates with a practical and locally adaptable mechanical anchorage system as an effective solution for the flexural strengthening and rehabilitation of existing reinforced concrete beams. This method represents an efficient and economical strengthening approach, particularly suitable for applications in resource-constrained environments.

6.1. Future Research Directions

Future studies should focus on the following areas:

- Durability of long-term prestressed CFRP systems, particularly under cyclic loading, temperature variations, and aggressive environmental conditions that are typical of bridge and infrastructure applications.
- Hybrid reinforcement systems involving more than one type of FRP (e.g., CFRP combined with basalt FRP or GFRP) to exploit the synergistic advantages in mechanical strength and ductility properties.
- Stress-free and self-locking anchorage systems aimed at reducing stress concentration effects and simplifying installation procedures in field applications.
- Full-scale structural verification, especially for bridge girders and deck systems, in order to evaluate scalability, fatigue performance, serviceability behavior, and economic feasibility.

6.2. Practical Implications

The findings of this study have direct practical significance for structural rehabilitation and strengthening:

- Prestressed CFRP retrofitting represents a minimally intrusive, high-performance, and corrosion-resistant strengthening technique suitable for deteriorating concrete bridges, beams, and slabs.
- The tested anchorage-based sandwich system ensures reliable stress transfer and reduces the risk of premature debonding, making it suitable for field implementation even where maintenance access is limited.
- The observed improvements in deflection control and crack reduction indicate that prestressed CFRP systems can restore or even exceed the serviceability performance of existing structures without introducing additional dead load.
- The study establishes a rational relationship between CFRP plate width and prestress level, providing a useful framework for optimization and potential guidance for future revisions of structural strengthening design codes.

The novelty of the present study lies in its systematic experimental investigation of reinforced concrete beams strengthened in flexure using CFRP plates, with particular emphasis on the influence of prestressing and plate width. The experimental methodology incorporates locally manufactured anchorage and prestressing systems, reflecting practical field conditions. Unlike many previous studies that focused primarily on analytical models or single-configuration experimental setups, the present work examines the combined influence of CFRP plate width and prestress level on flexural performance through comprehensive laboratory testing and controlled prestressing procedures.

The study also introduces a mechanical sandwich anchorage system designed to promote uniform stress transfer and minimize premature bond failure, an aspect that has received limited attention in previous research. The results demonstrate that a prestress ratio of 23% can significantly increase the ultimate load-carrying capacity, providing a valuable reference for the development of future design recommendations and strengthening guidelines. Furthermore, the use of locally available materials and cost-effective fabrication techniques highlights the potential of this approach for rehabilitating infrastructure in Iraq and other developing regions, supporting sustainable and context-specific retrofit solutions.

7. Declarations

7.1. Author Contributions

Conceptualization, Y.S.K. and AH.Z.; methodology, Y.S.K. and AH.Z.; validation, A.H.Z.; formal analysis, A.H.Z.; investigation Y.S.K.; resources, Y.S.K.; data curation, A.H.Z.; writing—original draft preparation, Y.S.K.; writing—review and editing, A.H.Z.; visualization, Y.S.K.; supervision, A.H.Z.; project administration, A.H.Z.; funding acquisition, Y.H.K. All authors have read and agreed to the published version of the manuscript.

7.2. Data Availability Statement

The data presented in this study are available on request from the corresponding author.

7.3. Funding

The authors received no financial support for the research, authorship, and/or publication of this article.

7.4. Conflicts of Interest

The authors declare no conflict of interest.

8. References

[1] Akbarpour, A., Volz, J., & Vemuganti, S. (2024). An Experimental Study Incorporating Carbon Fiber Composite Bars and Wraps for Concrete Performance and Failure Insight. Journal of Composites Science, 8(5), 174. doi:10.3390/jcs8050174.

[2] Jalil, A., & Al-Zuhairi, A. H. (2022). Behavior of Post-Tensioned Concrete Girders Subject to Partially Strand Damage and Strengthened by NSM-CFRP Composites. Civil Engineering Journal, 8(7), 1507–1521. doi:10.28991/CEJ-2022-08-07-013.

[3] Woo, S. K., Kim, J. H. J., & Byun, K. J. (2012). Development of strength prediction method of RC beams strengthened with prestressed CFRP plates by cross-section analysis. KSCE Journal of Civil Engineering, 16(6), 1011–1022. doi:10.1007/s12205-012-1471-2.

[4] Ibrahim, R. S., & Al-Zuhairi, A. H. (2022). Behavior of RC columns strengthened by combined (CFRP and steel jacket). Materials Today: Proceedings, 61, 1126–1134. doi:10.1016/j.matpr.2021.10.514.

[5] Garden, H. N., & Hollaway, L. C. (1998). An experimental study of the failure modes of reinforced concrete beams strengthened with prestressed carbon composite plates. Composites Part B: Engineering, 29(4), 411–424. doi:10.1016/S1359-8368(97)00043-7.

[6] Xue, W., Tan, Y., & Zeng, L. (2008). Experimental studies of concrete beams strengthened with prestressed CFRP laminates. PCI Journal, 53(5), 70–85. doi:10.15554/pcij.09012008.70.85.

[7] Barros, J. A. (2009). Pre-stress technique for the flexural strengthening with NSM-CFRP strips. FRPRCS-9 Sydney, Australia.

[8] Deng, J., Lee, M. M. K., & Li, S. (2011). Flexural strength of steel–concrete composite beams reinforced with a prestressed CFRP plate. Construction and Building Materials, 25(1), 379–384. doi:10.1016/j.conbuildmat.2010.06.015.

[9] Altaee, M. J. M. (2011). Effect of CFRP Plate Location on Flexural Behavior of RC Beam Strengthened with CFRP Plate. International Journal on Advanced Science, Engineering and Information Technology, 1(6), 592. doi:10.18517/ijaseit.1.6.119.

[10] Kang, K., Zhang, P., & Liu, F. T. (2012). Experiment Research of Flexural Behavior of Reinforced RC Beams Strengthened with the External Prestressed CFRP Plates. Advanced Materials Research, 466–467, 225–228. doi:10.4028/www.scientific.net/amr.466-467.225.

[11] Ghafoori, E., Motavalli, M., Botsis, J., Herwig, A., & Galli, M. (2012). Fatigue strengthening of damaged metallic beams using prestressed unbonded and bonded CFRP plates. International Journal of Fatigue, 44, 303–315. doi:10.1016/j.ijfatigue.2012.03.006.

[12] Rezazadeh, M., Ramezansefat, H., & Barros, J. (2016). NSM CFRP Prestressing Techniques with Strengthening Potential for Simultaneously Enhancing Load Capacity and Ductility Performance. Journal of Composites for Construction, 20(5). doi:10.1061/(asce)cc.1943-5614.0000679.

[13] Oudah, F., & El-Hacha, R. (2012). Fatigue behavior of RC beams strengthened with prestressed NSM CFRP rods. Composite Structures, 94(4), 1333–1342. doi:10.1016/j.compstruct.2011.11.025.

[14] Yang, J., Haghani, R., & Al-Emrani, M. (2019). Innovative prestressing method for externally bonded CFRP laminates without mechanical anchorage. Engineering Structures, 197, 109416. doi:10.1016/j.engstruct.2019.109416.

[15] Jeong, Y., Kim, W. S., Gribniak, V., & Hui, D. (2019). Fatigue behavior of concrete beams prestressed with partially bonded CFRP bars subjected to cyclic loads. Materials, 12(20), 3352. doi:10.3390/ma12203352.

[16] Sabah Abdulhameed, S. (2019). Strengthening of Concrete Beams with Prestressed FRP Reinforcements. Journal of Engineering and Sustainable Development, 2019(01), 13–25. doi:10.31272/jeasd.23.1.2.

[17] Hashim, H. A., & Al-Zuhairi, A. H. (2021). Effect of External Post-Tensioning Strengthening Technique on Flexural Capacity of Simple Supported Composite Castellated Beam. E3S Web of Conferences, 318, 3006. doi:10.1051/e3sconf/202131803006.

[18] Yang, J., Johansson, M., Al-Emrani, M., & Haghani, R. (2021). Innovative flexural strengthening of RC beams using self-anchored prestressed CFRP plates: Experimental and numerical investigations. Engineering Structures, 243, 112687. doi:10.1016/j.engstruct.2021.112687.

[19] Rogowski, J., & Kotynia, R. (2022). Comparison of Prestressing Methods with CFRP and SMA Materials in Flexurally Strengthened RC Members. Materials, 15(3), 1231. doi:10.3390/ma15031231.

[20] Liu, G., Li, B., Bao, J., Cheng, S., Meng, Q., & Zhao, S. (2023). Case Study on Prestressed CFRP Plates Applied for Strengthening Hollow-Section Beam Removed from an Old Bridge. Polymers, 15(3), 549. doi:10.3390/polym15030549.

[21] Tang, W. (2023). A review on flexural behavior of reinforced concrete beams strengthened with prestressed carbon fiber reinforced polymer plates. Journal of Physics: Conference Series, 2608(1), 12004. doi:10.1088/1742-6596/2608/1/012004.

[22] Chang, X., Wang, X., Liu, C., Huang, H., Zhu, Z., & Wu, Z. (2023). Parametric analysis on the flexural behaviour of RC beams strengthened with prestressed FRP laminates. Structures, 47, 105–120. doi:10.1016/j.istruc.2022.11.054.

[23] Shen, Y., Jiang, X., Qiang, X., & Chen, L. (2023). Experimental Study on Steel–Concrete Composite Beams Strengthened by Externally Prestressed CFRP Strips. Prestress Technology, 27(01), 39–52. doi:10.59238/j.pt.2023.01.004.

[24] Li, W., & Long, X. (2023). Research on the Application of Prestressed CFRP in Strengthening Concrete Beams. International Journal of Frontiers in Engineering Technology, 5(4). doi:10.25236/ijfet.2023.050406.

[25] Qi, H., Jiang, H., Wang, B., & Zhuge, P. (2024). Experimental Study on Shear Performance of Concrete Beams Reinforced with Externally Unbonded Prestressed CFRP Tendons. Fibers, 12(3), 23. doi:10.3390/fib12030023.

[26] Abbas, H. Q., & Al-Zuhairi, A. H. (2022). Usage of EB-CFRP for Improved Flexural Capacity of Unbonded Post-Tensioned Concrete Members Exposed to Partially Damaged Strands. Civil Engineering Journal (Iran), 8(6), 1288–1303. doi:10.28991/CEJ-2022-08-06-014.

[27] Wang, H. T., Liu, S. S., Shi, J. W., Xu, G. W., Chen, M. S., & Bian, Z. N. (2024). Bonded and unbonded strengthening of RC beams with the prestressed CFRP plate system: An experimental study. Construction and Building Materials, 438, 137118. doi:10.1016/j.conbuildmat.2024.137118.

[28] Ayad, T., Benhouria, A., & Rezigua, A. (2025). Improved theoretical study of stress behavior of reinforced concrete beam strengthened by prestressed carbon fiber reinforced polymer plates. Journal of Adhesion, 1–36. doi:10.1080/00218464.2025.2583295.

[29] Sharifi Ghalehnoei, M., & Noormohammadi, N. (2025). Finite Element Investigation of the Flexural Performance of RC Beams with Various Dimensions Strengthened Using Prestressed CFRP Sheets. International Journal of Concrete Structures and Materials, 19(1). doi:10.1186/s40069-025-00839-4.

[30] Lv, Y., Teng, Y., Li, X., Liu, J., Lu, C., & Zhang, C. (2025). The Analysis of Axial Compression Performance of Reinforced Concrete Columns Strengthened with Prestressed Carbon Fiber Sheets. Infrastructures, 10(8), 210. doi:10.3390/infrastructures10080210.

[31] Chen, X., Yang, G., Zhuo, J., Zhang, Y., Ren, C., Qi, L., Du, H., & Bu, C. (2024). Experimental study on large-scale compression members strengthened with circumferential prestressed CFRP plate. Heliyon, 10(6), 26995. doi:10.1016/j.heliyon.2024.e26995.

[32] Gong, S., Su, M., Zhang, J., & Peng, H. (2024). Flexural behavior of reinforced concrete beams strengthened with gradually prestressed near surface mounted carbon fiber-reinforced polymer strips under static and fatigue loading. Advances in Structural Engineering, 27(7), 1234–1250. doi:10.1177/13694332241246374.

[33] Qasim, M., Lee, C. K., & Zhang, Y. X. (2023). Flexural strengthening of reinforced concrete beams using hybrid fibre reinforced engineered cementitious composite. Engineering Structures, 284, 115992. doi:10.1016/j.engstruct.2023.115992.

[34] Attari, N., Amziane, S., & Chemrouk, M. (2012). Flexural strengthening of concrete beams using CFRP, GFRP and hybrid FRP sheets. Construction and Building Materials, 37, 746–757. doi:10.1016/j.conbuildmat.2012.07.052.

[35] El-Hacha, R., & Rizkalla, S. H. (2004). Near-surface-mounted fiber-reinforced polymer reinforcements for flexural strengthening of concrete structures. ACI Structural Journal, 101(5), 717–726. doi:10.14359/13394.

[36] Niu, H., & Wu, Z. (2006). Effects of FRP-Concrete Interface Bond Properties on the Performance of RC Beams Strengthened in Flexure with Externally Bonded FRP Sheets. Journal of Materials in Civil Engineering, 18(5), 723–731. doi:10.1061/(asce)0899-1561(2006)18:5(723).

[37] Slaitas, J., Valivonis, J., & Rimkus, L. (2020). Evaluation of stress-strain state of FRP strengthened RC elements in bending. Fracture mechanics approach. Composite Structures, 233, 111712. doi:10.1016/j.compstruct.2019.111712.

[38] Hadhood, A., Agamy, M. H., Abdelsalam, M. M., Mohamed, H. M., & Aly El-Sayed, T. (2019). Shear strengthening of hybrid externally-bonded mechanically-fastened concrete beams using short CFRP strips: Experiments and theoretical evaluation. Engineering Structures, 201, 109795. doi:10.1016/j.engstruct.2019.109795.

[39] Hadi, S., kazeminezhad, E., & safakhah, S. (2022). Full-scale experimental evaluation of flexural strength and ductility of reinforced concrete beams strengthened with various FRP mechanisms. Structures, 43, 1160–1176. doi:10.1016/j.istruc.2022.07.011.

[40] Abdoli, M., & Mostofinejad, D. (2024). Theoretical Analysis of Behavior of FRP-Strengthened Reinforced Concrete Members Subjected to Combined Torsion and Biaxial Bending. Journal of Composites for Construction, 28(3). doi:10.1061/jccof2.cceng-4397.

[41] Aprile, A., & Benedetti, A. (2004). Coupled flexural-shear design of R/C beams strengthened with FRP. Composites Part B: Engineering, 35(1), 1–25. doi:10.1016/j.compositesb.2003.09.001.

[42] Yang, J. Q., Liu, B., & Feng, P. (2025). Ductile behaviour of prestressed CFRP plate strengthened RC beams: Concept and experimental verification. Engineering Structures, 337, 120548. doi:10.1016/j.engstruct.2025.120548.

[43] Badawi, M., & Soudki, K. (2009). Flexural strengthening of RC beams with prestressed NSM CFRP rods - Experimental and analytical investigation. Construction and Building Materials, 23(10), 3292–3300. doi:10.1016/j.conbuildmat.2009.03.005.